Preliminary Cooling Channel Design in a Bimodal Nuclear Propulsion System Operating with Ammonia

Alberto Tacchi[1a], Stefano Giuntini[2b], Stefano Mannucci[2c], Elia Puccinelli[2d], Guido Francesco Frate[1e], Angelo Pasini[2f] and Lorenzo Ferrari[1g]

[1] Dept. of Energy, System, Territory and Construction Engineering, Pisa, Italy,
[2] Dept. of Civil and Industrial Engineering, Pisa, Italy,
[a] alberto.tacchi@phd.unipi.it (CA), [b] stefano.giuntini@phd.unipi.it, [c] stefano.mannucci@phd.unipi.it,
[d] elia.puccinelli@phd.unipi.it, [e] guido.frate@unipi.it, [f] angelo.pasini@unipi.it, [g] lorenzo.ferrari@unipi.it.

Abstract:

Nuclear-thermal and nuclear-electric propulsion (NTP and NEP, respectively) systems have been investigated as viable applications for nuclear reactors in space since the 1950s. Bimodal systems combine the high thrust of NTP with the high efficiency of NEP, using a single reactor. In the concept considered here, ammonia (NH_3) is adopted as a common fluid, acting as propellant for both the NTP and NEP engines, and working fluid for onboard power generation. However, openly available studies on ammonia thermo-hydraulics at nuclear-propulsion-relevant conditions—particularly across two-phase, near-critical and supercritical regimes—remain scarce, motivating a dedicated channel design. The proposed reactor concept features three channel families: (i) moderator channels enabling ammonia evaporation upstream of NTP operation, (ii) NTP thrust channels in a Particle Bed Reactor (PBR) arrangement, and (iii) power-generation (PG) channels that heat ammonia for a power conversion cycle.

The study provides preliminary sizing for the moderator evaporation and the PG channels, while the NTP thrust channel is deferred. Key outputs include feasible operating windows and preferred regimes that satisfy pressure-drop and thermal-margin constraints. The resulting channel layouts support stable operation across NTP/NEP switching and offer a scalable baseline for future coupled neutronic–thermal optimisation and system-level trade studies.

Keywords:

Thermo-hydraulics; Nuclear; Ammonia; Space; Cooling channels.

1. Introduction

The bimodal nuclear propulsion system proposed in the Bimodal Ammonia Nuclear Thermal Electric Rocket (BANTER) project combines thermo-nuclear (NTP) and nuclear-electric (NEP) propulsion systems [1]. In the former, the propellant, heated by the reactor core, increases its internal energy, which is then transformed into kinetic energy by the propellant expansion in a convergent-divergent nozzle to generate the thrust to propel the spacecraft. In the latter, the thermal power generated by the nuclear reactor heats a working fluid of a thermodynamic cycle to generate the electrical power for the electric thrusters.

The present work outlines a design methodology and the preliminary results for the thermo-hydraulic analysis for the cooling channels of a nuclear reactor to be used for space applications operating with ammonia. The final design of the cooling channels must guarantee continuous operation throughout the whole mission duration. Typical mission scenarios are identified in order to derive thermo-hydraulic requirements and constraints. A preliminary design of the moderator and power generation cooling channels is given.

The methodology adopted in the present work is useful to get a preliminary sizing of the cooling channels for an application that is quite unique in the literature, due to the propulsion system bimodality, the use of ammonia, the size constraints that are typical of space applications, and the low-gravity implications on the design.

1.1. Cooling channels

The nuclear reactor core designed for the BANTER mission features a composite cooling system architecture, comprised of three distinct channel configurations. These channels are classified based on their purpose:

- **Thrust Channels**: These channels include a nuclear fuel particle bed. The propellant flowing through these channels absorbs high-grade heat directly from the fuel and is subsequently routed to the graphite plate integrated converging-diverging nozzle for expansion, thereby generating the thrust [2].
- **Power Generation (PG) Channels**: These annular channels surround the NTP thrust channels. The working fluid cools both the inner channels, where the nuclear fuel is stored, and the outer moderator. The heated flow exits the reactor and expands through a turbine. Finally, the working fluid completes a thermodynamic cycle to generate the electrical power required for onboard subsystems.
- **Moderator Channels**: These channels cross the moderator matrix, the medium responsible for slowing fast neutrons to the thermal energy regime. Their role is to cool the solid moderator while evaporating the ammonia before it flows into the thrust channels.

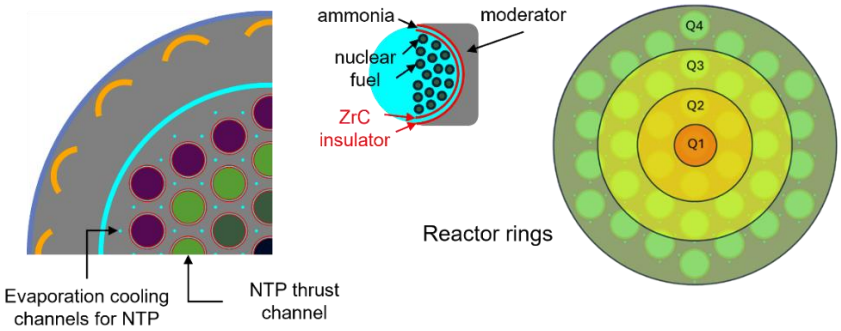

Figure 1.1. Example of reactor configuration (left), reactor rings for different power levels (right).

The reactor is subdivided into four rings, as shown in Figure 1. The power density increases from the outer to the inner rings. While moderator channels for ammonia evaporation are placed within the beryllium moderator, power-generation channels surround the NTP thrust channels. Hence, within a given reactor ring, the heat source intensity differs between the PG and the evaporation channels. Moreover, a different number of coolant channels is envisaged in the reactor for the two channel types.

1.2. Operating conditions

Considering the bimodal nature of the system, the design of the first prototype has been developed by considering two operating conditions:

- During the NTP burns ("**NTP-mode**"): Ammonia flows both inside the NTP thrust channels and the annular PG channels, while the reactor reaches its peak power level (Figure 2, left).
- When the NTP system is switched off ("**NEP-mode**"): Electric thrusters are operated. There is no ammonia flow inside the NTP channels. The power level produced by the fuel is lower than the previous case. However, flow in the annular channel is no longer assisted by the central ammonia flow (Figure 2, right).

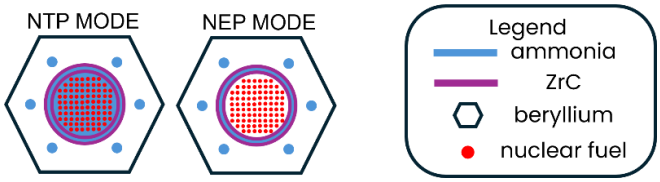

Figure 1.2. Schematic of the two operating modes to be considered for the heat transfer problem.

Regarding the evaluation of the heat transfer coefficient in low-gravity, the effect of low local accelerations may result in additional uncertainties on the quantitative evaluation of the heat transfer performance [3]. Kew and Cornwell recommended using the confinement number, $Co = \sigma/(a(\rho_l - \rho_v)D_h^2)^{0.5}$, as a criterion to differentiate macroscale and microscale two-phase flow and heat transfer.

Kew and Cornwell reported that the heat transfer and flow characteristic are significantly different than those observed in macrochannels for $Co > 0.5$ [4]. In fact, the evaluation of the confinement number on the proposed channels suggests that, especially for PG channels during NEP operation, these channels, which are macro channels in terrestrial conditions, become micro-channels during the space mission [5], since the NEP thrust is low with respect to the spacecraft mass, causing the local acceleration to reach $10^{-5}g$, which makes the confinement number to exceed 0.5. However, since there is no systematic approach to be applied (as confirmed by Celata [3]), and it is out of the scope of the present work to delve further into micro-gravity considerations, PG channels will be treated with the classical correlations of macro channels. This level of

detail is considered acceptable for system analysis and design. However, additional uncertainties are likely to be present.

The supercritical regime, where the pressure is higher than the critical pressure, is governed by a sharp non-linear behaviour of the thermophysical properties. In particular, the pseudo-critical line (or Widom line) is defined as the locus of points where the specific heat reaches its local maximum for a given pressure. Here, the fluid undergoes rapid changes in thermophysical properties, a phenomenon that originates from non-linear variations in the heat transfer coefficient [6]. Under these conditions, experimental data often show two phenomena around the pseudo-critical line: the Enhanced Heat Transfer (EHT), and the Deteriorated Heat Transfer (DHT). At low heat fluxes, the measured HTC may exceed theoretical values, usually calculated according to a Dittus-Boelter correlation (EHT), while at high heat fluxes, a degradation in performance (DHT) occurs. Unlike the abrupt wall temperature spike seen in subcritical Departure from Nucleate Boiling (DNB), DHT is characterized by a smoother, more gradual temperature increase, driven mainly by buoyancy and flow acceleration effects [7].

1.3. Moderator and power generation channels

The moderator channels are driven by two primary thermodynamic objectives:

- **Active Thermal Management**: To ensure that the beryllium moderator matrix remains within thermal safety margins, local temperatures must be kept below the phase-transition temperature, as beryllium undergoes an HCP–BCC transition at approximately 1520–1550 K (with melting occurring at 1560–1564 K). This transition must be avoided to prevent mechanical stress and swelling.
- **Regenerative Phase Change**: To exploit the deposited heat for pre-heating and evaporation of the propellant. The channels are specifically sized to bring high-pressure subcritical ammonia from a defined subcooled inlet state to a fully vaporised (saturated or superheated) state at the outlet, thereby avoiding the generation of phase-change-related instabilities in the thrust channels.

In the considered analysis the reactor in NTP-mode operates at a nominal power of 50 MW which, from neutronic simulations, deposits a power density of 8.6 MW/m^3 in the moderator. The core architecture consists of 111 distinct cooling channels distributed across four concentric rings within a 60 cm long reactor core. The channels are aligned longitudinally (parallel to the reactor axis), and the coolant can be directed in co-flow or counter-flow configurations, moving from the reactor inlet to the nozzle or vice versa. The computational domain is defined by an irregular shape shown on the left of Figure 1.3, which, for simplicity, is represented by a fluid duct, enclosed by an equivalent annular section of the beryllium moderator, maintaining the same area as represented on the right figure, which acts as the volumetric heat source. To satisfy the constraint of complete vaporisation at the outlet, the design accommodates multi-pass configurations, effectively increasing the residence time and heat transfer area if a single pass proves insufficient. In this analysis, the multipass configurations $(n_{passes} \geq 2)$ are implemented such that the moderator area per individual channel remains constant. This approach is effectively equivalent to increasing the reactor size as the number of channels increases. Consequently, the present analysis provides, as an output, the moderator power density (or total power) requirements necessary to vaporize the ammonia completely. This parameter will be useful for the subsequent coupled neutronic-TH simulations.

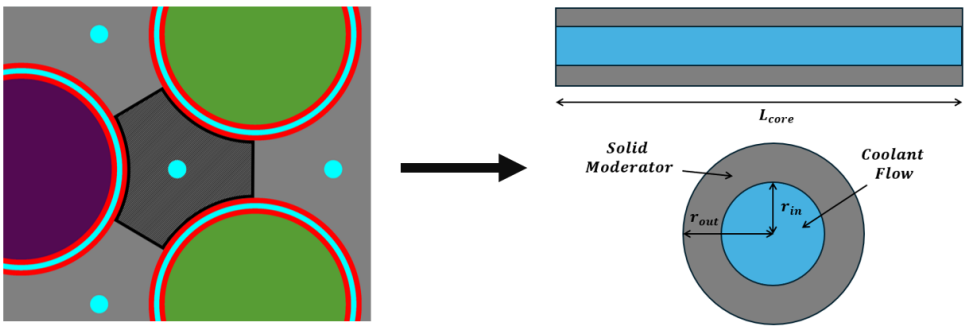

Figure 1.3. Layout of moderator channel for ammonia evaporation.

The power generation (PG) annular channels are designed to:

- Absorb heat from the NTP thrust channels and transfer it outside the reactor, ensuring an acceptable temperature profile on the inner walls.
- Guarantee the required electrical power output for the spacecraft subsystems – including electric pumps, electric thrusters, and all the other onboard loads – through an innovative power-conversion system.

Power generation channels have an annular shape and are concentric with the internal thrust channels.

Figure 1.3 depicts three annular channels for PG around a central moderator channel for ammonia vaporization, while Figure 1.4 depicts a cross-section of one annular channel. The ammonia passage is in light blue. The number of PG channels is equal to the number of thrust channels, which are 1, 6, 12, and 18, respectively, for rings 1, 2, 3, and 4. Regarding the heat-transfer model, the most relevant operating condition is considered first. Hence, the first step is to solve the heat-transfer problem when the NTP engine is switched off, namely in "NEP-mode". In NEP mode, the nuclear reactor develops about 1 to 3 MW of thermal power, calculated by assuming a power generation requirement of 300 kWe, with an expected conversion efficiency of 10 to 30%. In the control volume considered, the main heat source is the inner region ($r < r_{in}$), where the nuclear fuel is stored, where the peak Power Density (PWD) is about $100\,W/cm^3$. The volumetric heat-generation rate from the moderator ($r > r_{out}$) is two orders of magnitude lower than the one developed in the nuclear fuel, around $1\,W/cm^3$; therefore, at this stage, only the contribution of the nuclear fuel is considered. Accordingly, it is assumed that all the heat produced in the fuel is absorbed by the annular ammonia flow. An adiabatic boundary condition is imposed at the outer wall of the PG coolant channel, at $r = r_{out}$, which also defines the outer boundary of the control volume (see Figure 1.4 below).

The code couples the thermo-hydraulic analyses to the power generation system by considering different configurations of the power conversion cycle. The power conversion cycle is designed to generate a target power level of 300 kWe. Two power conversion cycles are considered, both of them closed, one with a pump-nuclear reactor-turbine-radiator set, and another with the addition of a regenerator at the turbine outlet to preheat the working fluid before entering the reactor. The parametric analyses identified two sets of configurations, based on different inlet/outlet conditions for the nuclear reactor. Each cycle configuration is characterized by a certain thermal-to-electric conversion efficiency, and a required mass flow. The cycle analysis also determined the reactor outlet expected conditions. By comparing the results obtained in the thermo-hydraulic analysis, it is possible to reconfigure the power conversion cycle to more realistic conditions.

The simulation imposes the prescribed PWD in each ring of the nuclear reactor, and, based on the fluid conditions at each axial location, evaluates heat transfer performance. The outputs of this analysis are the coolant temperature and pressure profiles, as well as the wall-temperature profile. The coolant exit conditions are used to iterate with the power conversion cycle analysis, while the wall temperature profile is used to assess potential material degradation.

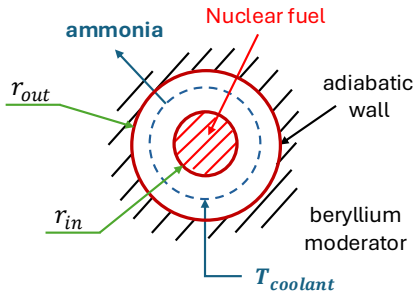

Figure 1.4. Scheme of a cross section of the control volume considered in the model for the heat transfer in PG channels.

2. Design methodology

A one-dimensional thermo-hydraulic framework (depicted in Figure 2.1) is developed with reactor heat generation prescribed as an input. The model explicitly resolves rapid thermo-physical property variations and flow-regime transitions and applies regime-dependent correlations to predict pressure losses, heat-transfer limits, and wall-temperature margins, including two-phase evaporation in the moderator and near/super-critical behaviour in PG channels.

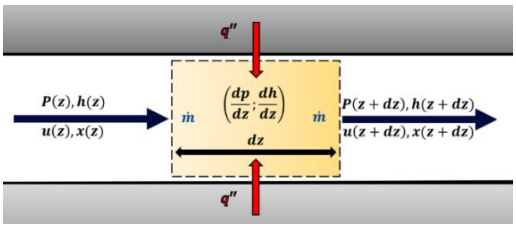

Figure 2.1. Schematics of thermo-hydraulic analysis of cooling channels (PG channels are heated only on the inner wall).

Two operating scenarios are assessed, where the reactor thermal power density and coolant boundary conditions differ markedly. During NTP burns, ammonia flows through the thrust channels cooling the nuclear fuel particles by forced convection; when the NTP engine is off, these channels experience no propellant flux, and the core heat generation primarily drives the thermal field.

2.1. Assumptions of the Thermo-Hydraulic model

The thermal-hydraulic analysis is governed by the following set of assumptions, equations and boundary conditions:

- Heat-transfer mechanisms inside the NTP thrust channel – between the nuclear fuel spheres and the wall –are not addressed here.
- Ammonia decomposition inside cooling channels due to pyrolysis and radiolysis is not considered yet.
- Channel instabilities due to parallel flow injection are not considered. Additional concentrated pressure drops at channel inlets shall be evaluated for refined designs [8].
- Steady-state condition: Transient effects are neglected ($\partial(\cdot)/\partial t = 0$).
- 1D flow model: The thermophysical properties of ammonia are assumed uniform across the channel cross-section (1-dimensional spatial discretisation along the axis).
- Homogeneous equilibrium model: In the two-phase regime, the liquid and vapour phases are assumed to flow at the same velocity and to be in thermodynamic equilibrium: $u_l(z) = u_v(z) = u_{TP}(z)\ and\ T_l(z) = T_v(z) = T_{TP}(z)$.
- Viscous flow: Friction and acceleration pressure losses are included, whereas hydrostatic pressure drops due to local spacecraft accelerations are neglected.
- Solid conduction: Heat conduction within the moderator is modelled radially at each cross-section; axial conduction is neglected.
- Power density (PWD): The volumetric power density (PWD) profiles are obtained from propulsive and power generation requirements. The required power density is either the one needed to vaporize ammonia in moderator channels, or the one necessary to heat the working fluid of the PG channels enough to generate the required electrical power for each ring and is assumed identical for all channels within the same ring. In the PG channel design, for each configuration of the conversion cycle, the corresponding efficiency is used to determine the thermal power that the working fluid shall get when passing through the reactor, with the relation: $\dot{Q}_{total} = \dot{W}_{net}/\eta_{cycle}$. The resulting PWD, considered as uniform in each reactor ring, has been approximated based on preliminary, non-coupled neutronic calculations, and scales by an assumed factor of 0.8 from the innermost ring towards the next outer ring.
- Inlet constraints: For MOD channels, the flow first passes through the radiation shield and the reactor reflector, both modelled as zero-dimensional heat-exchangers, before entering the moderator, where the inlet conditions fix the subcooling temperature. Inlet conditions for PG channels are determined by coupling the results of the parametric analyses of the thermodynamic power conversion cycle with thermo-hydraulics.
- Mass-flow distribution: In MOD channels, volumetric heat power density is assumed to be uniform on the radial and on the azimuthal directions over the whole reactor, while the axial distribution of the heat source is considered having a purely sinusoidal shape with peak q'''_{peak}. Hence, the mass flow is equally distributed among all the cooling channels. PG channels flow management is described in Section 3.2.
- CoolProp library used for fluid properties [9].

2.2. Governing equations of the Thermo-Hydraulic model

The governing equations for the ammonia flowing in the control volumes are reported below. The continuity equation is written as:

$$u(z) = \frac{\dot{m}}{\rho(p,h) \cdot A_{flow}} \qquad \textit{Equation 2.1.}$$

And the momentum balance as:

$$\frac{dp}{dz} = \left(\frac{dp}{dz}\right)_{fric} + \left(\frac{dp}{dz}\right)_{acc} = -f \cdot \frac{\rho u^2}{2D_h} - \rho \cdot u \cdot \frac{du}{dz} \qquad \textit{Equation 2.2.}$$

Where, for two-phase flows, the two-phase mixture density and Reynolds number are: $\rho_{TP} = 1/[\,x/\rho_v + (1-x)/\rho_l]$, $1/\mu_{TP} = x/\mu_v + (1-x)/\mu_l$, $Re_{TP} = (\rho_{TP} \cdot u_{TP} \cdot D_h)/\mu_{TP}$; the Darcy friction factor for smooth channels is given by: $f = 64/Re$ if laminar, $f = 0.316 \cdot Re^{-0.25}$ if turbulent (Blasius). The Churchill model is used for rough tubes, with roughness $= 20\ \mu m$. At channel bends, concentrated pressure losses are calculated as $\Delta p_{bend} = K_{bend}\rho v^2(722.8\,Re^{-0.83} + 0.9)/2$, where $K_{bend} = 3/2$ for 180° turns [10]. The energy balance is computed as follows:

$$\frac{dh}{dz} = \frac{q''' A_{source}}{\dot{m}} \qquad \textit{Equation 2.3.}$$

The boundary conditions for the moderator channels are an external radius adiabatic $(\partial T_{MOD}(r = r_{ext})/\partial r) = 0$ and $T_{MOD}\ (r = r_{in}) = T_w$; whereas for PG channels, since the heat flux originates from the inner wall, the following conditions are considered: $q''(z, r = r_{in}) = (q'''(z, r = r_{in})\ A_{NTP-channel})/2\pi\, r_{in}$, $q''(z, r = r_{out}) = 0$, where: $A_{NTP-channel} = \pi\, r_{in}^2$. The heat flux is determined from the PWD: $q'' = (q''' \cdot A_{source})/P_{wet}$, and the equilibrium quality: $x = (h - h_l)/(h_v - h_l)$.

For the convective single-phase heat transfer the Gnielinski correlation is implemented, which is generally valid for Reynolds numbers greater than 3000 and less than $5 \cdot 10^6$, and Prandtl numbers between 0.5 and 2000 . Regarding the two-phase heat transfer, the Klimenko formulation is applied using the equilibrium quality [11]. The Klimenko formulation was chosen due to its adoption in similar studies for NTP with ammonia [12], and for its agreement with the few experimental data available using ammonia [13], [14]. As suggested by Nikitaeva [12], in this approach, suitable values for the local acceleration of the spacecraft were used in the equation of the capillary length. In particular, the order of magnitude of the acceleration is estimated to be around $10^{-5} g$ for NEP operation, and about $10^{-1} g$ during NTP burns. As suggested by Di Marco, Celata e Zummo [15], these acceleration levels are in accordance with the literature. To physically determine the transition point where the heat transfer mechanism shifts from pure single-phase convection to subcooled nucleate boiling, the model utilizes the Davis & Anderson criterion [16], looking for the value of T_{wall} that triggers the Onset Nucleate Boiling (ONB) phenomenon. The Dougall–Rohsenow (DR) correlation is employed in this work to estimate the convective heat-transfer coefficient during forced convection of a liquid–vapor mixture in the cooling channels after the verification of the Critical Heat Flux (CHF) condition [17]. The CHF is used to denote the conditions at which the heat transfer coefficient of the two-phase flow substantially deteriorates. In a system in which the heat flux is independently controlled, the consequences of the CHF occurrence is the rapid rise in the wall temperature [20], as it will be seen in Sections 3.1 and 3.2. The formulation of DR is particularly suitable for boiling flows in ducts, where the liquid phase remains predominantly dispersed and the vapor phase plays a dominant role as quality is approaching unity (dry-out phenomenon). The assumption is that the vapor phase governs the behaviour of the mixture, while the liquid contributes primarily through its presence as entrained droplets or thin films. As a result, the effective Reynolds number of the mixture can be expressed as a vapor-based Reynolds number corrected for the local vapor quality.

In the vapor phase, at $x > 1$, the Gnielinski model is again the one assumed for heat transfer between the wall and the bulk. When the pressure exceeds the critical pressure, the algorithm automatically switches its correlation to the Dittus-Boelter model, where the convective heat transfer is calculated as in [18]. While literature suggests that Dittus-Boelter correlation may over- or under-predict HTC near the pseudo-critical point, it serves as a reliable first-order approximation for supercritical ammonia, as done in Cheng et al. [18]. It should be noted that specific corrections for EHT and DHT phenomena have not yet been implemented in the current development stage; however, their integration is planned for future updates to enhance the predictive accuracy of the code.

As concerning the adoption of the most appropriate correlations for the case of annular channels, the thermal boundary conditions are specified, prescribing the heat flux conditions at the inner wall of the duct. Heat transfer regimes are strongly dependent on the thermal boundary condition in the laminar flow regime, while very much less dependent in the turbulent flow regime for fluids with $Pr > 1$. Hence, the thermal boundary conditions, though applicable also to turbulent flows, are useful mainly for laminar flows [19]. For the mono-phase regions (liquid or vapor) of the flow in the annular channels we will therefore take advantage of the solutions reported in Shah and London, when the flow is laminar [19]. In order to obtain preliminary results, the hydrodynamic as well as thermal profiles are assumed to be completely developed. The solutions are written as a function of the outlet to the inlet annular channel radii $r^* = r_{out}/r_{in}$ and give, based on the radii ratio r^*, both the Darcy friction factor, as a function of the Reynolds number, and the Nusselt number at the inner wall of the annular channel. As concerning turbulent regimes and two-phase flow, the same correlations used for moderator circular channels are adopted.

3. Results

3.1. Moderator channel analysis for evaporation

The TH mass flow rate within the moderator channels is determined by the engine's thrust-to-weight optimization requirements. To evaluate the moderator channels performance, analyses were conducted using a total ammonia mass flow rate ranging from 5 to 20 kg/s, distributed across parallel channels arranged in the reactor rings. Within the engine cycle, the ammonia is initially stored at 20 bar with 2 K of subcooling. An onboard pump (with $\eta_{pump} = 0.8$) elevates the fluid to an operating pressure between 70 and 100 bar. Before

entering the moderator, the coolant passes sequentially through the radiation shield and the reflector, effectively reducing the degree of subcooling. The key design objective for the moderator is to achieve complete evaporation of ammonia ($x \geq 1$) at the channel outlet, while containing the pressure drops. The output is the required volumetric power density peak q'''_{peak}, which must be compatible with the actual heat deposition rate achievable in the beryllium moderator matrix from neutron and gamma heating. Figure 3.1 summarizes the parametric behaviour of the system. In the figure (a) the required peak volumetric power density decreases strongly with increasing number of channels, as the thermal duty is distributed over a larger total heat-transfer area. This effect is particularly pronounced when there are few channels, where the thermal load per channel is high, for the reference reactor including 111 channels the required power density is 51.63 MW/m^3 at 80 bar for $\dot{m}$ =11.9 kg/s. However, increasing the number of channels, maintaining the moderator area fixed the beryllium volume increase monotonously. In figure (b) the pressure drop decreases with increasing D_h, as expected from classical friction scaling, especially after D_h higher than 8 mm. However, this is accompanied by a reduction in mass flux G, which may degrade heat transfer performance. Therefore, the design space is governed by a trade-off between thermal feasibility and hydraulic constraints. The combined effect of pump outlet pressure and peak volumetric power density is illustrated in the figure (c), where contours of outlet equilibrium quality are reported. The map clearly identifies a favourable design region in which complete evaporation can be achieved. Increasing the pump outlet pressure at 100 bar shifts this region toward lower required power densities, as the latent heat of vaporization decreases with pressure, thereby reducing the total enthalpy rise needed to reach vapor conditions (q'''_{peak}=46.61 MW/m^3). Conversely, decreasing the system pressure at 70 bar increases the latent heat requirement, even if the subcooling temperature is decreased, leading to higher power densities such as 53.36 MW/m^3 for complete evaporation. As a result, low-pressure operation becomes progressively less favourable from a thermal standpoint, unless compensated by an increase in heat-transfer surface by increasing the number of channels or passes. The detailed axial distributions for a representative configuration are shown in Figure 3.2. In the representative two-pass configuration, the bulk temperature increases from subcooled conditions to saturation, with the onset of nucleate boiling marking the transition to the two-phase regime. The vapor quality then increases progressively toward the outlet, where a temperature of approximately 405 K is reached, consistent with the requirements of the downstream thrust channels. The pressure drop remains limited, indicating that the design is primarily governed by thermal rather than hydraulic constraints. However, near the end of the second pass, a pronounced deterioration of the HTC transfer coefficient is observed, accompanied by an unavoidable sharp increase in wall temperature, which nevertheless remains below the threshold limit ($T_{wall}^{threshold}$) of 1000 K.

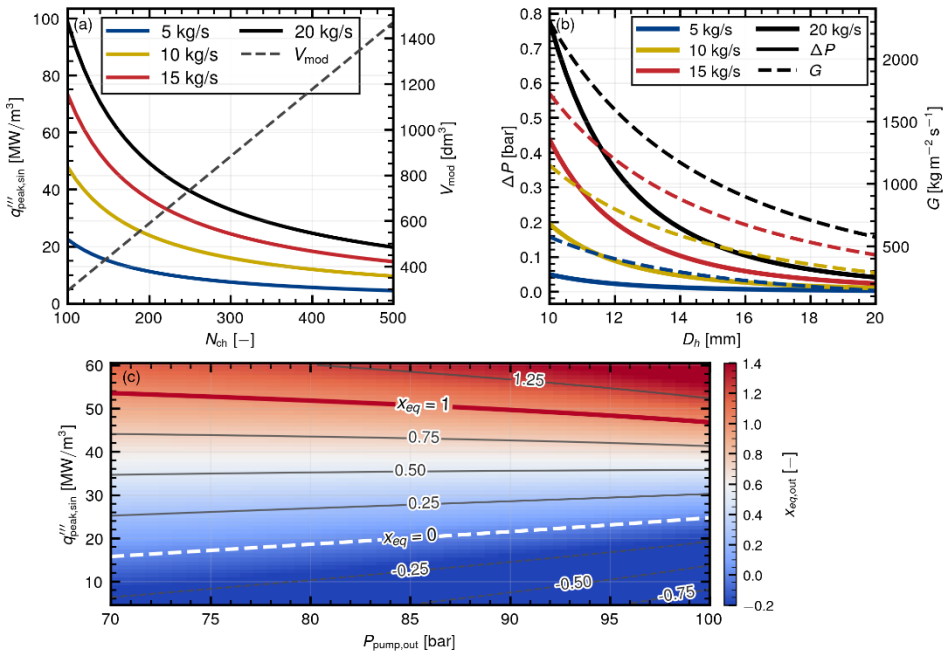

Figure 3.1. (a) PWD requirements vs moderator N_{ch} (D_h=14mm, $p_{pump,out}$=80 bar). (b) Δp and G vs D_h at full vapor (N_{ch}=111, $p_{pump,out}$=80 bar). (c) x_{out} vs q''' and $p_{pump,out}$ (N_{ch}=111, D_h=14mm).

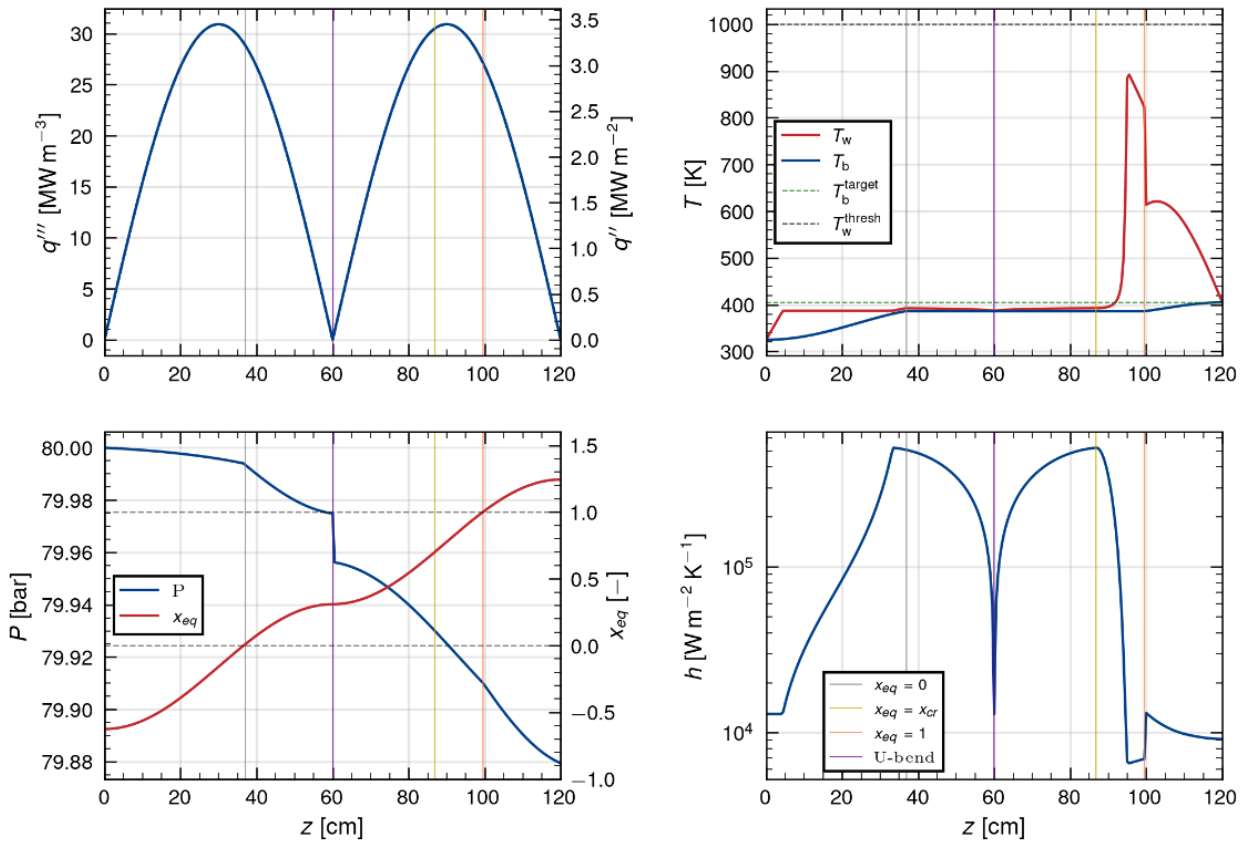

Figure 3.2. Distributions of heat source (top left), temperature (top right), pressure and quality (bottom left), and HTC (bottom right) for moderator channels (D_h = 14 mm, n_{passes}=2, $\dot{m}$=11.9 kg/s).

This behaviour highlights the onset of the dry out regime at high vapor quality. Therefore, achieving complete evaporation alone is not sufficient, and the design must also ensure that local wall-temperature peaks remain within acceptable limits. This preliminary sizing can therefore be interpreted as a direct requirement for the neutronic design, since the currently available deposited power density remains below the 26 MW/m^3 required by the TH analysis to achieve complete evaporation at the reference mass flow rate. In this sense, the moderator results establish the target increase in local power deposition that future coupled neutronic–TH optimizations must deliver.

3.2. Power generation channels analysis to match Power Cycle

As anticipated in Section **Errore. L'origine riferimento non è stata trovata.**, the PG channel design is made by coupling the power conversion cycle parametric analysis with the thermo-hydraulic model during NEP-mode. In the cycle parametric analysis, the reactor outlet temperature and the pump outlet pressure are varied respectively between 600 and $800\ K$, and between 90 and $150\ bar$. In the case without recuperation (pump-reactor-turbine-radiators), the pump outlet coincides with the reactor inlet; in the recuperated cycle (pump-regenerator-reactor-turbine-regenerator-radiators), the regenerator outlet coincides with the reactor inlet. The power conversion cycle analysis assumes the reactor as a constant heat source, and determines an expected reactor outlet temperature $T_{reactor}^{outlet}$ (shown in Table 3.1). In this simulation, the temperature of the inner wall, which is made of ZrC (zirconium carbide), of the annular PG channel is calculated. As a first approximation, considering the inherent uncertainty of the model, the maximum acceptable value for the inner wall temperature is set to $T_{wall}^{threshold} = 1100\ K$. The inner radius of the annular channel is constrained by the dimension of the thrust channel, and is equal to $r_{in} = 5\ cm$, while the outlet radius r_{out} can be varied. For PG channels, the number of channels is constrained. Moreover, the inherent high thermal PWD developed in the reactor causes, on average, an early verification of the Critical Heat Flux (CHF) condition for the flow, which degrades heat transfer performance of the two-phase flow, possibly resulting in unacceptable wall temperature profiles if single-pass strategies are adopted. Hence, the working fluid is firstly directed into the outermost ring of the reactor, where the PWD is at its lowest, and then it is directed progressively towards the innermost ring of the reactor. The objective is to cover as much distance as possible before reaching the CHF condition.

Table 3.1. Power conversion cycle configurations considered in the analysis.

Configurations			**Without regenerator**				**With regenerator**			
ID	$T_{reactor}^{outlet}$	p_{pump}^{outlet}	$p_{reactor}^{inlet}$	$T_{reactor}^{inlet}$	η_{cycle}	$\dot{m}_{tot}$	$p_{reactor}^{inlet}$	$T_{reactor}^{inlet}$	η_{cycle}	$\dot{m}_{tot}$
[-]	[K]	[bar]	[bar]	[K]	[-]	[kg/s]	[bar]	[K]	[-]	[kg/s]
1	600	90	90	296	0.18	0.91	88	360	0.22	0.93
2	600	120	120	297	0.20	0.85	118	350	0.23	0.86
3	600	150	150	298	0.21	0.82	147	342	0.24	0.82
4	700	90	90	296	0.20	0.74	88	391	0.26	0.76
5	700	120	120	297	0.22	0.68	118	387	0.27	0.69
6	700	150	150	298	0.23	0.65	147	381	0.28	0.65
7	800	90	90	296	0.20	0.63	88	391	0.29	0.64
8	800	120	120	297	0.22	0.57	118	407	0.31	0.58
9	800	150	150	298	0.24	0.54	147	410	0.32	0.55

First, one sixth of the total mass flow $\dot{m}_i = \dot{m}_{tot}/6$ – with $\dot{m}_{tot}$ estimated by the analysis of the power conversion cycle – passes through three consecutive channels on the outermost Ring 4. Second, this mass flow $\dot{m}_i$ enters the next inner Ring 3, where it passes through two subsequent channels. Third, the mass flow $\dot{m}_i$ passes through one channel of Ring 2. Each sixth $\dot{m}_i$ of the original total mass flow $\dot{m}_{tot}$ follows the same path and reaches the innermost Ring 1, where there is only one channel available. Here, it is assumed that all the six $\dot{m}_i$ reach Ring 1 in the same conditions. Finally, at Ring 1, all the six mass flows $\dot{m}_i$ are collected together and enter the last single channel before exiting the reactor.

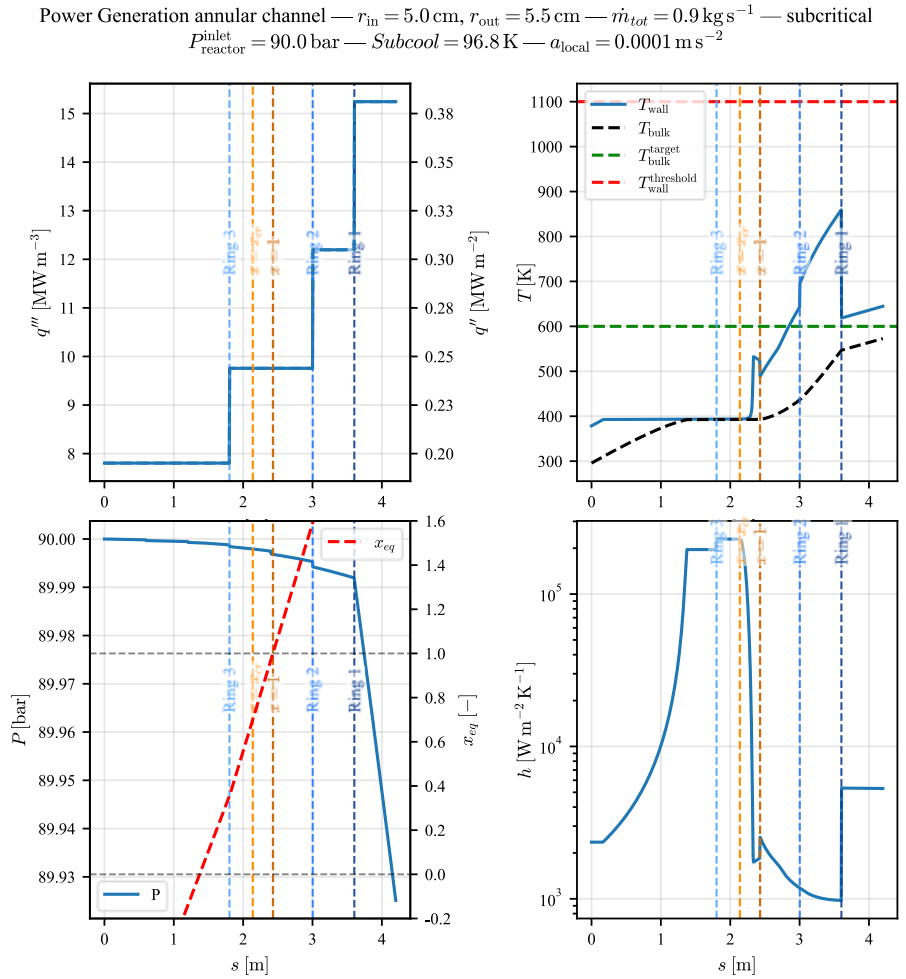

Figure 3.3. PGS serial path – symmetric leg + final Ring 1. Evolutions of PWD and heat flux (top left), temperature (top right), pressure and quality (bottom left), and HTC (bottom right) for PG channels, ID 1 configuration of Table 3.1.

The reactor PWD is assumed to be uniform in each ring, and scales by a factor of 0.8 at each step towards the next outer ring. Once all the simulations are run, the reactor outlet temperature calculated by the TH model

is compared to the one foreseen by the cycle analysis, and the wall temperature profile is checked against the threshold value. If the two values of the reactor outlet temperatures of the fluid are in accordance, and if the wall temperature does not exceed the threshold value of 1100 K, the configuration is considered to be successful. This wall temperature limit is conservative, since the material that must sustain this temperature is ZrC. However, due to the model uncertainties, it is considered as acceptable. An example of the results obtained from the simulations is shown in the Figure 3.3, for the case without regenerator, identified by ID 1 in Table 3.1. Here, the top-left subplot shows the reactor PWDs, in MW/m^3, calculated for that cycle configuration in each ring, assumed to be uniform on the channel length, which are necessary to heat up the working fluid to the target reactor outlet temperature T_{bulk}^{target}, needed to generate the target electrical power of $300\ kWe$. From the reactor inlet, at Ring 4, to the inlet of the last channel of Ring 1, the subplots show the path of one sixth of the total mass flow $\dot{m}_i = \dot{m}_{tot}/6$. Then, all the six sixths of the total mass flow enter the last single channel of Ring 1. The bottom-left subplot shows the evolution of the working fluid pressure and equilibrium quality along the aforementioned path. The bottom-right subplot depicts the calculated heat transfer coefficient (HTC) as the fluid progresses through the reactor. The enhancement of the HTC at Ring 4 is due to the onset of nucleate boiling, which promotes the best heat transfer performance. The subsequent decay in the HTC at Ring 3, instead, is due to the so-called Critical Heat Flux condition, where bubbles are not able to detach from the heated surface anymore, causing a deterioration of the heat transfer. After the HTC decay, the Dougall-Rosenhow (DR) correlation is adopted. When the flow becomes a vapor, at x=1, the model uses a different correlation, the Gnielinski one. Since the DR correlation is developed to be continuous only with the Dittus-Boelter correlation at x=1, the HTC shows a discontinuity. The HTC rises again at Ring 1, since all the mass flow is entering one channel that has the same flow passage of the previous channels, determining a higher flow velocity that, in turns, promotes a higher HTC. The bulk and wall temperature profiles are shown in the top-right subplot of Figure 3.3. The wall temperature is a result of the imposed heat flux and local HTC: it is the temperature that the wall must reach in order to guarantee that heat flux based on the local HTC. Here, we can observe the good agreement between the target reactor outlet temperature, T_{target}^{bulk}, calculated by the cycle analysis, with the bulk temperature at reactor outlet calculated by this thermo-hydraulic model. Also, the wall temperature is well below the maximum threshold value imposed $T_{wall}^{threshold}$. Finally, all the configurations are compared in the Figure 3.4-left for an annular geometry with $r_{in} = 5\ cm, r_{out} = 5.5\ cm$, where the temperature differences between the working fluid reactor outlet temperature predicted by the cycle and the one predicted by the thermo-hydraulic (TH) model are depicted against the objective of being within a temperature difference of 25 K degrees, which would not affect cycle performance significantly. Configuration with ID 7 with the regenerator showed a higher dispersion due a combination of effects. First, a higher reactor outlet temperature expected, of about 800 K, combined with the sub-critical inlet pressure, give an almost null subcooling degree at the reactor inlet (due to the regenerator), and the Critical Heat Flux is reached in the very first region of the channel. Second, the lower mass-flow promotes a lower heat transfer performance. This result suggests that situations of this kind must be furtherly evaluated, since the code may underestimate the reactor outlet temperature. The other configurations are all inside acceptable ranges, however, as the predicted reactor outlet temperature rises, the mismatch between the cycle and the TH model increases as well. However, the configurations without the regenerator with ID 7,8 and 9, namely all the ones that the cycle analysis predicted to have a reactor outlet temperature of 800 K, exceeded the threshold limit for the maximum wall temperature. While the bulk temperature mismatch at the reactor outlet is not influenced by a variation in the outer radius r_{out} of the annular channel from 5.5 cm to 6.0 cm, as shown by the comparison of Figure 3.4-left with Figure 3.4-right, the same assertion cannot be stated for the wall temperature profile, which is significantly affected by the variation of the outer radius of the annular channel. In fact, in the configuration with $r_{in} = 5.0\ cm$, $r_{out} = 6.0\ cm$ all the wall temperature profiles exceed the threshold limit of 1100 K.

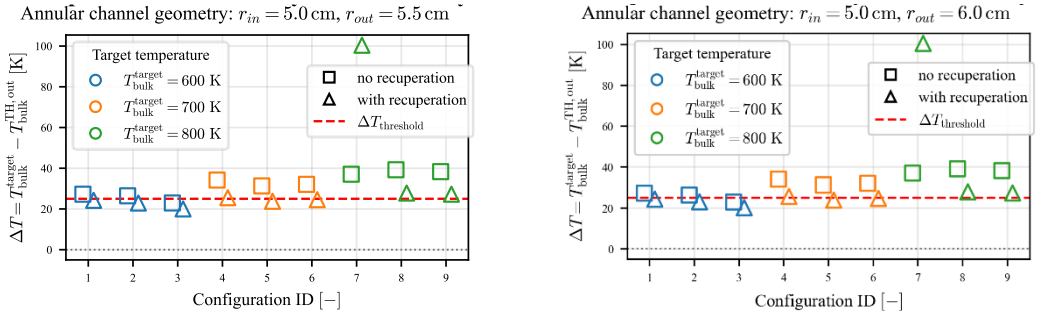

Figure 3.4. Temperature difference in [K] between the reactor outlet temperatures predicted by the cycle analysis, T_{target}^{bulk} and the thermo-hydraulic (TH) model, $T_{bulk}^{TH,out}$. Results are depicted for both the case with (triangles) and without (squares) recuperation for different target temperatures of the working fluid at the reactor outlet. Diagram on the left shows results for $r_{out} = 5.5\ cm$; diagram on the right for $r_{out} = 6.0\ cm$.

4. Conclusion

This work presented a preliminary thermo-hydraulic design methodology for ammonia cooling channels in a bimodal nuclear propulsion reactor, with specific focus on moderator evaporation channels and power-generation annular channels. The proposed framework captures the main thermal-hydraulic constraints associated with the two operating modes of the BANTER concept and provides a first sizing tool for identifying feasible channel layouts, operating pressures, and target thermal regimes.

For the moderator channels, the present analysis indicates that complete ammonia evaporation is achievable only within a limited design window, with the volumetric power density deposited in the beryllium matrix and the mass flow rate as the governing parameters. Higher pump outlet pressure reduces the enthalpy required for vaporization, while multi-pass layouts decrease the local power density by spreading the thermal duty over a larger heated length. Accordingly, multi-pass solutions are more promising than a single-pass layout, with the two-pass configuration representing a reasonable first compromise, pending further refinement through neutronic analysis. However, important limitations remain. Thermal interaction between adjacent channels was neglected, and although ammonia vaporization in moderator channels appears theoretically possible, the required peak power density may still exceed the level realistically achievable in the present configuration by simple power scaling. In addition, the outlet dry-vapor condition alone is not sufficient, since the wall-temperature peak near the outlet suggests that dryout-type behavior may become the actual limiting factor. A possible improvement could be the introduction of a solid fuel matrix around the vaporization channels, in a configuration closer to NERVA-type concepts, to increase the locally deposited power and make complete vaporization more feasible. Overall, the present results provide a preliminary sizing indication for the moderator channels, showing that the final design should reduce the heat load absorbed by each channel while increasing the power effectively deposited in the moderator, in order to make ammonia vaporization achievable within acceptable thermal margins.

For power generation channels, the objective of the analysis was to couple the thermo-hydraulic (TH) model with the power conversion parametric analysis in order to better understand the achievable temperature for the working fluid at the reactor outlet, and to compare it with the expected temperature from the cycle analysis. The preliminary TH analysis suggests that, for the annular channel with $(r_{in}, r_{out}) = (5.0, 5.5)\ cm$, in order to reach temperatures higher than 800 K at reactor outlet, the addition of the regenerator may be crucial to reach the prescribed temperature, while not exceeding the wall temperature limit. However, the addition of the regenerator must be furtherly evaluated since, at sub-critical pressures, the fluid might encounter the Critical Heat Flux early, and may not reach the desired temperature for the conversion cycle. This behaviour may be due to numerical uncertainties and hence further works will address the issue. If lower temperatures than 800 K are required, even configurations without recuperation can give promising results.

Acknowledgments

The authors would like to thank Prof. Di Marco from the University of Pisa for his helpful feedbacks, and for sharing his expertise about reactor design in low-gravity environments. The project leading to this paper has received funding from the European Union's research and innovation programme under agreement No 101186520. BANTER, Bimodal Ammonia Nuclear Thermal and Electric Rocket.

Nomenclature

h specific enthalpy J/kg
$\dot{m}$ mass flow rate, kg/s
T temperature, K
p pressure, bar
f friction factor, -
k thermal conductivity, W/(m K)
q'' heat flux, W/m^2
q''' volumetric thermal power density, W/m^3
D_h hydraulic diameter, m
σ surface tension, J/m^2
Co confinement number, -
$\dot{Q}$ thermal power, W
u velocity, m/s
r radius, m
z axis, m
η efficiency
a acceleration, m/s^2
Co confinement number, -
u velocity, m/s

Subscripts and superscripts:

G mass flux, kg/(m^2 s)

x equilibrium quality, -

ρ density, kg/ m^3

P perimeter, m

A area, m^2

a acceleration, m/s^2

SP single-phase

TP two-phase

fg vaporization

out outer

in inner

References

[1] A. Pasini *et al.*, 'Bimodal Ammonia Nuclear Thermal and Electric Rocket (BANTER): Project Overview', in *IAF Space Propulsion Symposium*, Sydney, Australia: International Astronautical Federation (IAF), 2025, pp. 734–745. doi: 10.52202/083090-0080.

[2] E. Puccinelli and A. Pasini, 'Reduced-Order Model of Ammonia Decomposition Reaction for Increasing Nuclear Thermal Rocket Performance', in *IAF Space Power Symposium*, Sydney, Australia: International Astronautical Federation (IAF), 2025, pp. 445–454. doi: 10.52202/083089-0045.

[3] G. P. Celata, *Heat Transfer and Fluid Flow in Microchannels*. Begell House Inc., 2004. doi: 10.1615/978-1-56700-208-9.0.

[4] P. A. Kew and K. Cornwell, 'Correlations for the prediction of boiling heat transfer in small-diameter channels', *Appl. Therm. Eng.*, vol. 17, no. 8–10, pp. 705–715, Aug. 1997, doi: 10.1016/S1359-4311(96)00071-3.

[5] P. Di Marco, 'Review of Reduced Gravity Boiling Heat Transfer: European Research', *Eur. Res.*, vol. 20, no. 4, 2003.

[6] F. Li, B. Pei, and B. Bai, 'Heat Transfer Correlations of Supercritical Fluids', in *Advanced Supercritical Fluids Technologies*, I. Pioro, Ed., IntechOpen, 2020. doi: 10.5772/intechopen.89356.

[7] F. Nasuti and M. Pizzarelli, 'Pseudo-boiling and heat transfer deterioration while heating supercritical liquid rocket engine propellants', *J. Supercrit. Fluids*, vol. 168, p. 105066, Feb. 2021, doi: 10.1016/j.supflu.2020.105066.

[8] C.-J. Kuo and Y. Peles, 'Pressure effects on flow boiling instabilities in parallel microchannels', *Int. J. Heat Mass Transf.*, vol. 52, no. 1–2, pp. 271–280, Jan. 2009, doi: 10.1016/j.ijheatmasstransfer.2008.06.015.

[9] K. Gao, J. Wu, I. H. Bell, A. H. Harvey, and E. W. Lemmon, 'A Reference Equation of State with an Associating Term for the Thermodynamic Properties of Ammonia', *J. Phys. Chem. Ref. Data*, vol. 52, no. 1, p. 013102, Mar. 2023, doi: 10.1063/5.0128269.

[10] I. A. Pasini, E. Puccinelli, M. Uchiumi, and D. Nakata, 'Modeling of Tank Emptying and Injector Discharge Coefficient in a Self-Pressurized System of a Hybrid Rocket'.

[11] V. V. Klimenko, 'A generalizes correlation for two-phase forced flow heat transfer'.

[12] D. Nikitaeva, 'Nikitaeva, Daria, "Implications of alternative in-situ propellants used in nuclear thermal propulsion engines" (2021). Dissertations. 231. https://louis.uah.edu/uah-dissertations/231'.

[13] G. Barthau, 'EXPERIMENTAL INVESTIGATION OF CONVECTIVE BOILING OF AMMONIA AT HIGH PRESSURES', *M M O N A*.

[14] H. Wang and X. Fang, 'Evaluation Analysis of Correlations of Flow Boiling Heat Transfer Coefficients Applied to Ammonia', *Heat Transf. Eng.*, vol. 37, no. 1, pp. 32–44, Jan. 2016, doi: 10.1080/01457632.2015.1025006.

[15] G. P. Celata and G. Zummo, 'FLOW BOILING HEAT TRANSFER IN MICROGRAVITY: RECENT PROGRESS', *Multiph. Sci. Technol.*, vol. 21, no. 3, pp. 187–212, 2009, doi: 10.1615/MultScienTechn.v21.i3.20.

[16] N. E. Todreas and M. S. Kazimi, 'Nuclear systems. 1: Thermal hydraulic fundamentals / Neil E. Todreas; Mujid S. Kazimi', 2. printing., New York: Taylor & Francis, 1993.

[17] V. P. Carey, 'Liquid-Vapor Phase-Change Phenomena'.

[18] X. Cheng, B. Kuang, and Y. H. Yang, 'Numerical analysis of heat transfer in supercritical water cooled flow channels', *Nucl. Eng. Des.*, vol. 237, no. 3, pp. 240–252, Feb. 2007, doi: 10.1016/j.nucengdes.2006.06.011.

[19] R. K. Shah and A. L. London, *Laminar flow forced convection in ducts: a source book for compact heat exchanger analytical data*. in Advances in heat transfer : Supplement, no. 1. New York: Academic Press, 1978.